

# Molecular Evolution from AGB Stars to Planetary Nebulae

Sun Kwok<sup>1</sup>

<sup>1</sup>Faculty of Science, The University of Hong Kong, Hong Kong, China  
email: [sunkwok@hku.hk](mailto:sunkwok@hku.hk)

**Abstract.** The late stages of stellar evolution from the Asymptotic Giant Branch (AGB) to planetary nebulae represent the most active phase of molecular synthesis in a star's life. Over 60 molecular species, including inorganics, organics, radicals, chains, rings, and molecular ions have been detected in the circumstellar envelopes of evolved stars. Most interestingly, complex organic compounds of aromatic and aliphatic structures are synthesized over very short time intervals after the end of the AGB. Also appeared during the post-AGB evolution are the unidentified 21 and 30  $\mu\text{m}$  emission features, which are believed to originate from carbonaceous compounds.

The circumstellar environment is an ideal laboratory for the testing of theories of chemical synthesis. The distinct spectral behavior among AGB stars, proto-planetary nebulae (PPN), and planetary nebulae (PN) and the short evolutionary time scales that separate these stages pose severe constraints on models. In this paper, we will present an observational summary of the chemical synthesis in the late stages of stellar evolution, discuss chemical and physical processes at work, and speculate on the possible effects these chemical products have on the Galaxy and the Solar System.

---

## 1. Introduction

An intermediate mass (1-8  $M_{\odot}$ ) star undergoes H and He shell burning after having developed a C-O electron-degenerate core. The luminosity and size of the star increase continuously as the star climbs the asymptotic giant branch (AGB) on the Hertzsprung-Russell diagram. At the same time, a stellar wind commences and gradually reduces the mass of H envelope. Over the last one million years of AGB evolution, up to several solar masses of circumstellar envelope can be built up by this mass loss process. This large-scale mass loss terminates when the entire H envelope is depleted. Continued H-shell burning will further deplete the remaining H envelope, giving the appearance of the star evolving to higher effective temperatures while maintaining a constant luminosity. This is the beginning of the post-AGB phase of evolution. When the stellar temperature reaches 30,000 K, the stellar Lyman continuum output is high enough to photoionize the circumstellar envelope, creating a planetary nebula. A detailed description on the origin and evolution of planetary nebulae can be found in Kwok (2000).

Manifestations of the mass loss process include the observation of rotational and vibrational transitions of molecules, and the vibrational modes of solid particles. The stellar wind in the AGB phase is expanding at  $\sim 10 \text{ km s}^{-1}$ , giving a dynamical age of the circumstellar envelope of  $\sim 10^4 \text{ yr}$ . From stellar evolution models, the transition from the end of AGB to the beginning of PN is about several thousand years and objects in this phase of evolution are called proto-planetary nebulae (PPNs, Kwok 1993). Accelerated by a later-developed fast wind, PNs expand at higher speeds ( $\sim 20\text{-}30 \text{ km s}^{-1}$ ), giving them a life time of 20,000-40,000 yr before being dispersed into the interstellar medium.

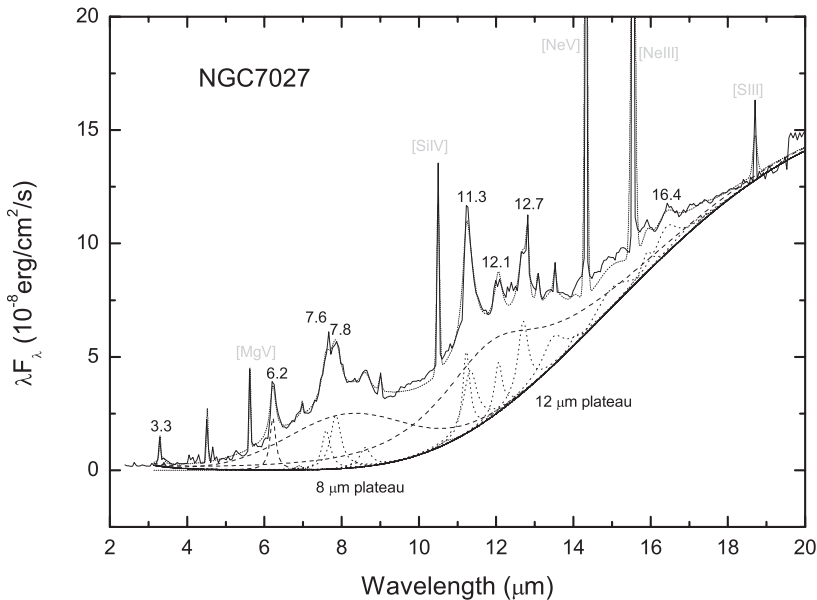


**Figure 1.** ISO spectrum of the planetary nebula NGC 7027. The thin solid lines are fits to discrete features and the dashed lines are fits to the plateau features.

The particle densities of the envelope are in the range of  $10^2 - 10^6 \text{ cm}^{-3}$ . It is in this low-density, rapidly changing environment that molecular synthesis is taking place.

## 2. Synthesis of molecules and dust in AGB and post-AGB evolution

The circumstellar envelopes of stars in the late stages of stellar evolution represent an ideal laboratory to study the formation of organic compounds. The process begins with the synthesis of the element carbon by the triple- $\alpha$  nuclear reaction in the core of AGB stars. The dredge up of this element to the surface allows the formation of simple carbon molecules such as  $\text{C}_2$ ,  $\text{C}_3$ ,  $\text{CN}$ , etc., in the photosphere. The initiation of a stellar wind during the late AGB stage results in the formation of gas-phase molecules in the outflow. Over 60 molecular species have been detected, and they include inorganics (e.g.,  $\text{CO}$ ,  $\text{SiO}$ ,  $\text{SiS}$ ,  $\text{NH}_3$ ,  $\text{AlCl}$ , etc.), organics ( $\text{C}_2\text{H}_2$ ,  $\text{CH}_4$ ,  $\text{H}_2\text{CO}$ ,  $\text{CH}_3\text{CN}$ , etc.), radicals ( $\text{CN}$ ,  $\text{C}_2\text{H}$ ,  $\text{C}_3$ ,  $\text{HCO}^+$ , etc.), chains (e.g.,  $\text{HCN}$ ,  $\text{HC}_3\text{N}$ ,  $\text{HC}_5\text{N}$ , etc.), and rings ( $\text{C}_3\text{H}_2$ ). Since the dynamical lifetime of the envelope is  $\sim 10^4$  yr, the chemical reactions that lead to the formation of these species must be shorter than this time scale. Interferometric observations also allow the mapping of the molecular emission regions and therefore put further constraints on the reaction zone (see Guélin, these proceedings).

Accompanying this molecular outflow is the condensation of solid-state species, the most common of which are amorphous silicates and silicon carbide, both have strong spectroscopic features in the mid-infrared (Kwok, Volk & Bidelman 1997). Near the end of the AGB, the mass loss rate of the star is so high that the star itself can be totally obscured by its circumstellar dust envelope. In carbon-rich AGB stars, the continuum is often featureless and amorphous carbon has been suggested as the carrier of the continuum. It is also in this stage that the  $13.7 \mu\text{m } \nu_5$  vibrational line of  $\text{C}_2\text{H}_2$  can be seen in absorption against the dust continuum (Volk, Xiong & Kwok 2000). In the post-AGB phase of evolution, lines of  $\text{C}_4\text{H}_2$ ,  $\text{C}_6\text{H}_2$  and  $\text{C}_6\text{H}_6$  appear (Cernicharo *et al.* 2001). The

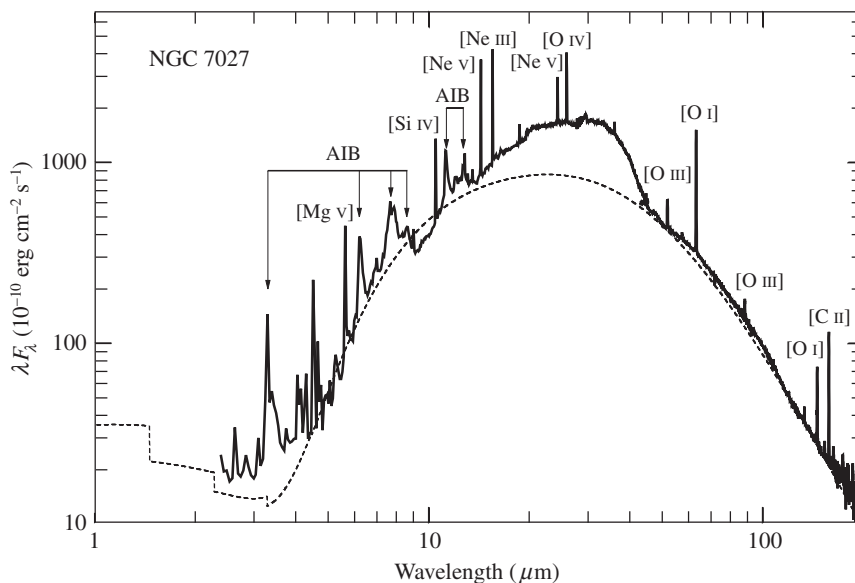


**Figure 2.** The *ISO SWS/LWS* spectrum of NGC 7027 between 1–200  $\mu\text{m}$ . Some of the stronger atomic lines and AIB features are marked. The dashed line is a model fit composed of a sum of dust emission, *f-b* and *f-f* gas emission. The excess in 2–5  $\mu\text{m}$  above the dashed line suggests that there is a warm dust component. The strong 30  $\mu\text{m}$  feature can be clearly seen above the dust continuum.

first sign of aromatic features appear in PPN. The 3.3, 6.2, 7.7, 8.6, and 11.3  $\mu\text{m}$  C–H and C–C stretching and bending modes of aromatic compounds can be seen in many C-rich PPN (Kwok, Volk & Hrivnak 1999, Hrivnak, Geballe & Kwok 2007). These aromatic infrared bands (AIB) are commonly found in C-rich PN and an example of PN spectrum is shown in Fig. 1.

### 3. Spectral features of PN and PPN

The infrared spectra of PPNs and PNs are characterized by the following characteristics:

- A strong continuum between 3 and 200  $\mu\text{m}$
- Aromatic features at 3.3, 6.2, 7.7, 8.6 and 11.3  $\mu\text{m}$ .
- Aliphatic features at 3.4 and 6.9  $\mu\text{m}$ .
- Other emission features at 15.8, 16.4, 17.4, 17.8 and 18.9  $\mu\text{m}$ .
- Plateau emission features at 8, 12, and 17  $\mu\text{m}$ .
- Unidentified broad emission features at 21 and 30  $\mu\text{m}$ .

These spectral properties are discussed in detail below.

*The infrared continuum.* All PPN and PN (O- or C-rich) possess a strong infrared continuum stretching from the near infrared to millimeter wavelengths (Fig. 2). The color temperature of this continuum is  $\sim 50$ –100 K for PNs and higher for PPNs (Zhang & Kwok 1991). This continuum is generally assumed to be due to the remnant of the dust envelope from the AGB phase. Quite often a separate higher temperature dust continuum is needed to fit the underlying broad emission in the near infrared region (Zhang, Kwok, & Hrivnak 2010). This “warm” component is likely to be created during the post-AGB evolution. Such a broad emission continuum can only be produced by micron-size

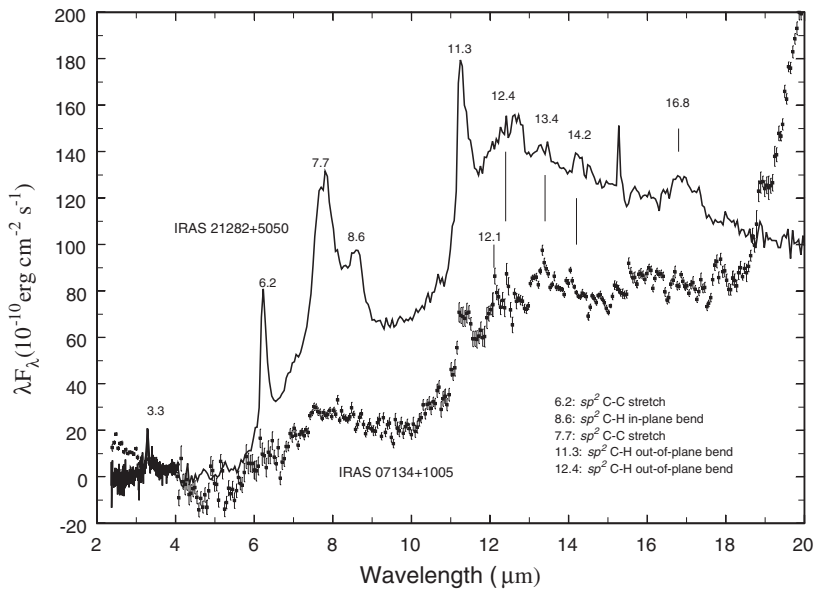


**Figure 3.** *ISO SWS01* spectra of the young PN IRAS 21282+5050 and the PPN IRAS 07134+1005, showing various aromatic C–H and C–C stretching and bending modes at 3.3, 6.2, 7.7, 8.6, and 11.3  $\mu\text{m}$ . Beyond the 11.3  $\mu\text{m}$  feature are the 12.1, 12.4, 13.3  $\mu\text{m}$  out-of-plane bending mode features from small aromatic units.

solid-state particles, although the particles sizes responsible for the near-infrared continuum are likely to be smaller.

*The aromatic infrared bands.* The infrared emission features at 3.3, 6.2, 7.7, 8.6, and 11.3  $\mu\text{m}$  are now firmly identified as arising from the stretching and bending modes of aromatic compounds (Knacke 1977, Duley & Williams 1981, Allamandola, Tielens & Barker 1989, Puget & Léger 1989) and they are collectively called the aromatic infrared bands (AIB).

*The 11.3, 12.1, 12.4, 13.3  $\mu\text{m}$  features* can be seen in the spectra of PPN (Fig. 3) and can be identified as C–H out-of-plane bending modes of aromatic units with different number of exposed corners. The 11.3, 12.1, 12.4, 13.3  $\mu\text{m}$  features correspond to a lone C–H group, two, three, or four adjacent C–H groups, respectively (Hudgins & Allamandola 1999).

*The 3.4 and 6.9  $\mu\text{m}$  features.* The infrared spectra of PPNs differ from PNs in that the 3.4  $\mu\text{m}$  feature can be as strong as the 3.3  $\mu\text{m}$  feature (Geballe *et al.* 1992). The 3.4  $\mu\text{m}$  feature has been identified as due to symmetric and antisymmetric stretching modes of methyl and methylene aliphatic groups, and these separate modes can be clearly identified (Hrivnak, Geballe & Kwok 2007). The 6.9  $\mu\text{m}$  feature is strong in PPN and has been attributed to aliphatic C–H bending modes (Kwok, Volk & Hrivnak 1999, Kwok, Volk & Bernath 2001).

*The 15.8  $\mu\text{m}$  feature.* The 15.8  $\mu\text{m}$  feature ( $\Delta\lambda \sim 1.3\mu\text{m}$ ) is strong in 21  $\mu\text{m}$  sources (Fig. 4) (Hrivnak, Volk & Kwok 2009, Zhang, Kwok, & Hrivnak 2010). Figure 5 shows a comparison of the profiles of the 15.8 and 21  $\mu\text{m}$  features.

*The 8 and 12  $\mu\text{m}$  plateau features.* In addition to hydrogen, methyl ( $-\text{CH}_3$ ) or methylene ( $-\text{CH}_2$ ) side groups, it is also possible that other side groups such as carbonyl ( $\text{C}=\text{O}$ ), aldehydic ( $-\text{HCO}$ ), phenolic ( $\text{OH}$ ), and amine ( $\text{NH}_2$ ) be attached to the

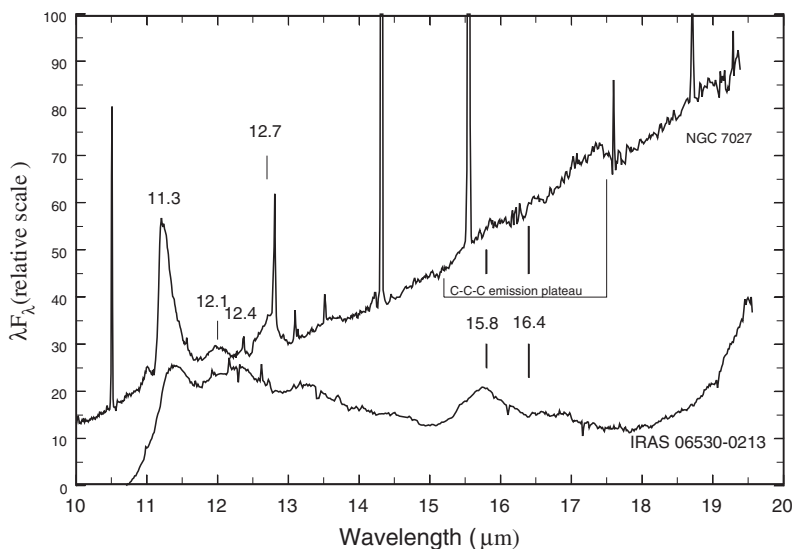


**Figure 4.** The *Spitzer* IRS spectra of young PN NGC 7027 and the PPN IRAS 06530–0213 showing 11.3, 12.1  $\mu\text{m}$  AIB features and the unidentified 15.8  $\mu\text{m}$  feature, and the 15–17.5  $\mu\text{m}$  emission plateau in NGC 7027. The narrow feature in the NGC 7027 are atomic lines.

aromatic units. The broad emission plateaus at 8 and 12  $\mu\text{m}$  are identified as superposition of in-plane and out-of-plane C–H bending modes of various aliphatic sidegroups attached to the aromatic rings (Fig. 6) (Kwok, Volk & Bernath 2001). Although these plateaus can be seen in the spectra of PN (Fig. 1), they are relatively more prominent in PPNs (Fig. 7).

*The 17  $\mu\text{m}$  plateau.* A very broad emission plateau extending from 15 to 20  $\mu\text{m}$  can be seen in the spectra of PPNs and PNs (Fig. 8). This feature has been suggested to be due to aromatic C–C–C in-plane and out-of-plane distortion modes (van Kerckhoven *et al.* 2000).

*The 21 and 30  $\mu\text{m}$  features.* The AIB features are not the only infrared emission features that emerge in the post-AGB evolution. A strong emission feature at 21  $\mu\text{m}$  was first discovered in four PPNs (Kwok, Volk & Hrivnak 1989) and is now seen in  $\sim 15$  post-AGB stars in the Galaxy and  $\sim 10$  in the Magellanic Clouds (Volk *et al.* 2011). High resolution *ISO* observations have shown that the 21  $\mu\text{m}$  feature to have no detectable subfeatures. The intrinsic profiles of the feature is found to have a consistent shape among different sources, peaking at  $\sim 20.1 \pm 0.1$   $\mu\text{m}$  (Fig. 9) (Hrivnak, Volk & Kwok 2009).

The unidentified emission feature around 30  $\mu\text{m}$  was first seen in carbon-rich AGB stars (e.g. IRC+10216 and AFGL 2688) and PN (Fig. 2). The 30  $\mu\text{m}$  feature is now found to be common among carbon-rich PPN, especially those showing the 21  $\mu\text{m}$  emission feature. This feature is very prominent in PNs and PPNs and is responsible for  $\sim 20\%$  of the total infrared emission (Hrivnak, Volk & Kwok 2000). The possibility that thiourea ( $\text{SC}(\text{NH}_2)_2$ ) and OH groups may contribute to the 30  $\mu\text{m}$  feature has recently been suggested (Papoular 2011).

#### 4. How do they form?

Although theoretically the condensation process is difficult to understand, observationally we see organics of aliphatic and aromatic structures form in PPNs on time scales

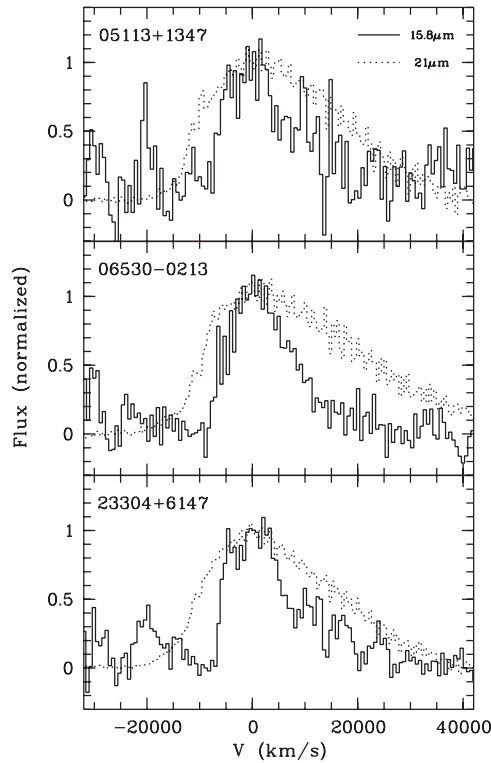


**Figure 5.** Comparison of the profiles of the 21 and 15.8  $\mu\text{m}$  features in 3 PPNs. Figure adapted from Zhang, Kwok & Hrivnak (2010).

as short as a few hundred years. The best evidence that for their ease of formation can be found in novae, where the aliphatic features appear on a time scale of days. Figure 10 shows the infrared spectrum of the nova V2362 Cygni. Its spectrum changed from a pure gas spectrum of one showing strong dust continuum on time scale of months or

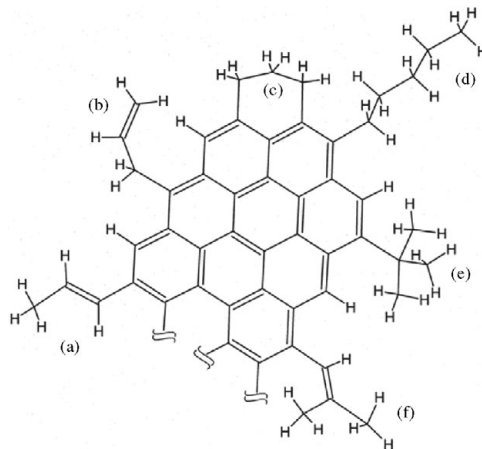


**Figure 6.** Schematic chemical structure illustrating the various possible side groups attached to aromatic rings that contribute to the plateau emissions (from Kwok, Volk & Bernath 2001).

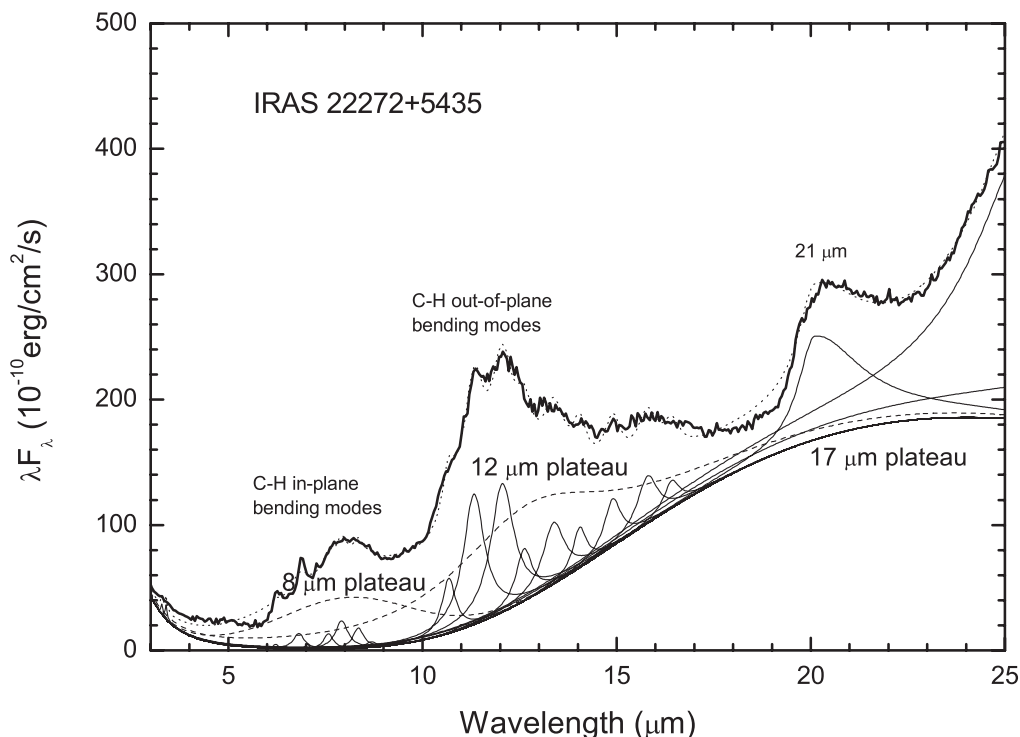


**Figure 7.** Spitzer IRS spectrum of the PPN IRAS 22272+5435. The thin solid lines are fits to discrete features and the dashed lines are fits to the plateau features. The rise at the long wavelength end is due to the 30  $\mu\text{m}$  feature. Although the AIBs can be seen, most of the fluxes are emitted in the 8 and 12  $\mu\text{m}$  plateau features and the 21 and 30  $\mu\text{m}$  features.

even days. A strong 8  $\mu\text{m}$  plateau feature is clearly evident in this spectrum. In the case of Nova V705 Cas, the 3.3, 3.4, 8.2, and 11.4  $\mu\text{m}$  can be seen to emerge in the nova spectrum less than a year after outburst (Fig. 11) (Evans *et al.* 2005).

A similar example can be found in the optical transient source in the galaxy NGC 300. The 8 and 12  $\mu\text{m}$  plateaus emissions can be seen about 3 months after outburst (Fig. 12).

## 5. Chemical structure of the carrier

Although the hypothesis that the AIB features originate from polycyclic aromatic hydrocarbons (PAH) molecules is popular in the astronomical community, there are a number of difficulties with this hypothesis. PAHs are fused ring molecules made up of C and H† and their vibrational bands are sharp and the peak wavelengths well defined. However, the observed UIE features are broad. In order to fit the observed astronomical spectra, it is necessary to use a complex mixture of PAHs of different sizes, structures, and charge states (Allamandola, Hudgins & Sandford 1999, Peeters *et al.* 2002), adopt empirical emission profiles (Draine & Li 2007), or a mixture of PAHs with each feature convolved with artificial profiles (Cami 2011). PAH molecules are primarily excited by

† In this conference, the term PAH (sometimes in quotation marks) is used to refer to various carbonaceous compounds containing both aromatic and aliphatic components. Since PAH is a precisely defined chemical term, it is the best if we end the confusion by confining the use of this term to fused aromatic rings.

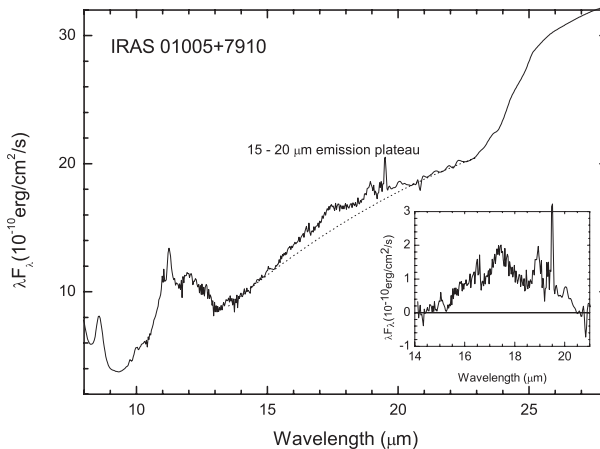


**Figure 8.** Spitzer IRS spectrum of the PPN IRAS 01105+7910 showing the 17  $\mu\text{m}$  plateau emission. Figure adapted from Zhang, Kwok & Hrivnak (2010).

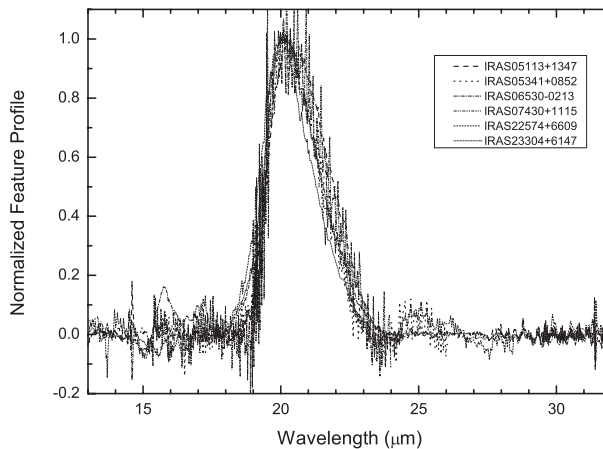


**Figure 9.** Comparison of the normalized 21  $\mu\text{m}$  feature profile from the *Spitzer* spectra of 6 PPN. The features all have the same intrinsic profile and peak wavelengths. Figure adapted from Hrivnak, Volk & Kwok (2009).

UV radiation but AIBs are seen in PPNs and reflection nebulae with low temperature central stars. The observed shapes and peak wavelengths of the AIBs are independent of stellar temperature (Uchida *et al.* 2000). Furthermore, in spite of the well known vibrational and rotational spectra of PAH molecules, no individual PAH molecule has ever been detected either in absorption or emission (Clayton *et al.* 2003, Pilleri *et al.* 2009).

These issues are particularly relevant in evolved objects as the 3.4 and 6.9  $\mu\text{m}$  aliphatic features and the 8 and 12  $\mu\text{m}$  plateau features are strong. These spectral properties are similar to those observed in natural substances such as coal (Papoular *et al.* 1989, Guillois *et al.* 1996), kerogen, and petroleum fractions (Cataldo, Keheyan & Heymann 2002, Cataldo & Keheyan 2003, Cataldo, Keheyan & Heymann 2004). A number of artificial substances synthesized in the laboratory can also be candidates of the carrier. Hydrogenated amorphous carbon (HAC, Jones *et al.* 1990) are produced by laser ablation of graphite in a hydrogen atmosphere (Scott & Duley 1996). Quenched carbonaceous composites (QCC) are produced by hydrocarbon plasma deposition (Sakata *et al.* 1987).

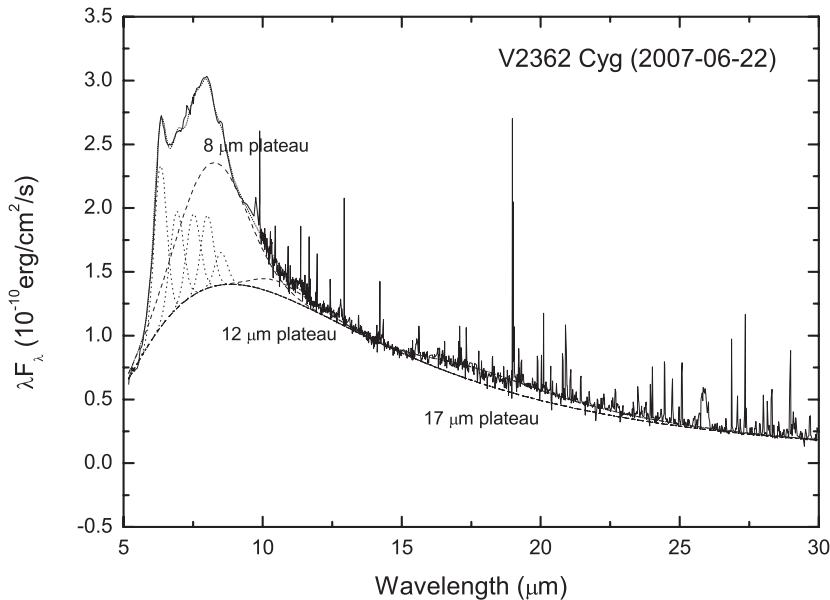


**Figure 10.** Spitzer IRS spectrum of nova V2362 Cygni at 446 days after outburst. A strong 8  $\mu\text{m}$  plateau feature can clearly be seen above the dust continuum. The dotted lines are fits to discrete features at 6.2, 6.9, 7.6, 7.8, and 8.6  $\mu\text{m}$ .

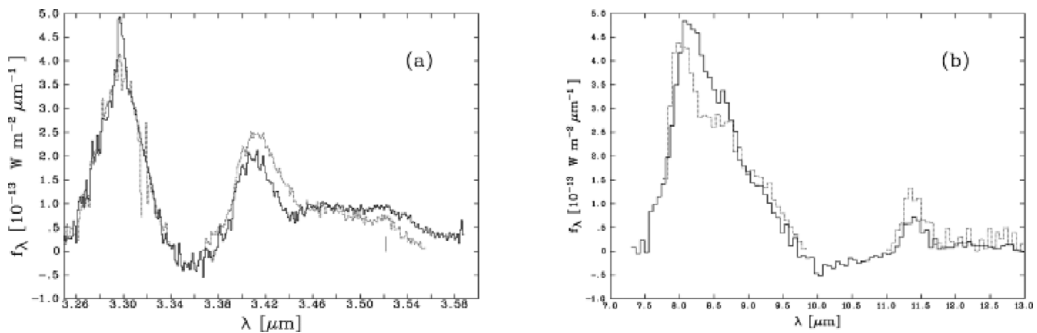


**Figure 11.** Profiles of the 3.3  $\mu\text{m}$  and 3.4  $\mu\text{m}$  features (left) and the 8.2  $\mu\text{m}$  and 11.4  $\mu\text{m}$  features (right) of Nova V705 Cas at two different epochs (253 and 320 days after outburst, shown as solid and broken lines respectively). Figure adapted from Evans *et al.* (2005).

Carbon nanoparticles of sizes 1-10 nm made up of primarily  $sp^2$  carbon rings connected by a network of aliphatic chains can be made under different conditions and different initial gaseous compositions (Colangeli *et al.* 1995, Duley & Hu 2009, Jäger *et al.* 2009). These are all amorphous solids made up of pure H and C. When N is introduced, other organic solids are possible. Tholins is a refractory organic material formed by UV photolysis of reduced gas mixtures ( $\text{N}_2$ ,  $\text{NH}_3$ ,  $\text{CH}_4$ ). HCN polymers are amorphous hydrogenated carbon nitride formed spontaneously from HCN.

We therefore suggest that the carrier of the UIE features in evolved stars are organic nanoparticles with mixed aromatic/aliphatic structures. The amorphous nature of the compound implies that there is a large variation of the bond lengths and bond angles, leading naturally to broad emission features. The small sizes of the particles will allow them to radiate in the near infrared region, and the mixed  $sp^2/sp^3$  structure can naturally explain the observed spectral features. An example of such structure is shown in Fig. 13.

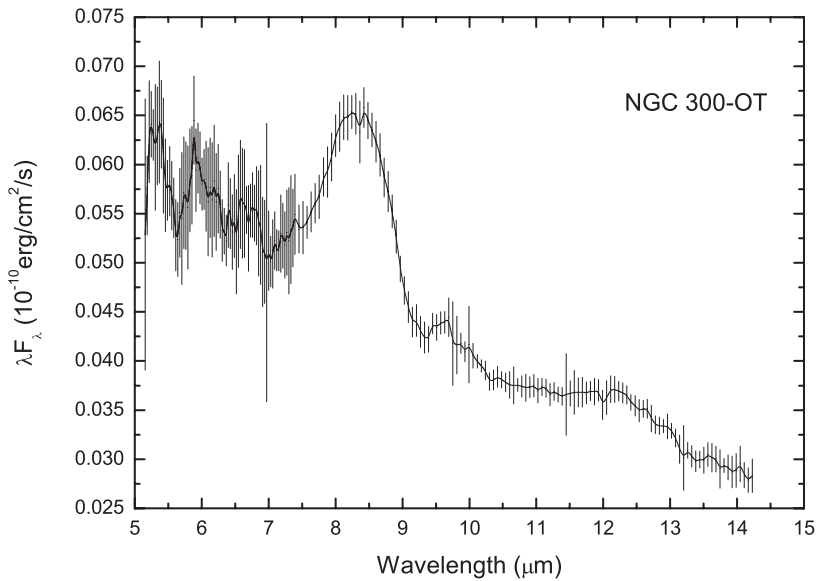


**Figure 12.** *Spitzer* IRS spectrum of the optical transient source NGC 300-OT 93 days after discovery. Broad emission features around 8 and 12  $\mu\text{m}$  can be seen. Figure adapted from Prieto *et al.* 2009.

## 6. The stellar-solar system connection

In spite of the common perception that Solar System bodies are made up of minerals, metals, and ices, organics are in fact abundantly present in meteorites, comets, asteroids, and interplanetary dust particles (IDPs). Over 70% of the organics in carbonaceous chondrite meteorites is in the form of insoluble organic matter (IOM, Alexander *et al.* 2007). IOM is a macromolecular material with structures similar to that of kerogen (Kerridge 1999) and is possibly of interstellar origin due to excess of D,  $^{13}\text{C}$ , and  $^{15}\text{N}$  (see Alexander, these proceedings). Samples returned from the Comet Wild 2 also contain a significant organic component (Sandford *et al.* 2006). Spectra of IDPs show the 3.4  $\mu\text{m}$  aliphatic feature and sometimes the C=O group (Flynn *et al.* 2003, Keller *et al.* 2004).

Using a variety of laboratory techniques such as Fourier transform infrared spectroscopy, nuclear magnetic resonance, electron paramagnetic resonance, X-ray absorption near-edge spectroscopy, high resolution electron microscopy, and thermal and chemical degradations, Derenne & Robert (2010) were able to determine the elemental and molecular contents of the Murchison IOM. A schematic of their model of the IOM is shown in Fig. 13. This structure is characterized by small units of aromatic islands and extensive aliphatic branches. Significant impurities such as O, N, and S atoms are also present.

## 7. Implications

We now know that PPNs and PNs are able to synthesize organic compounds of aromatic and aliphatic structures in the very low density circumstellar environment. The chemical structure of these organics undergo changes over time scales of hundreds of years. It is possible that photochemistry plays a part in this chemical evolution. Two unidentified emission features at 21 and 30  $\mu\text{m}$  are observed. It is likely that these are carbonaceous compounds of unusual chemical compositions.

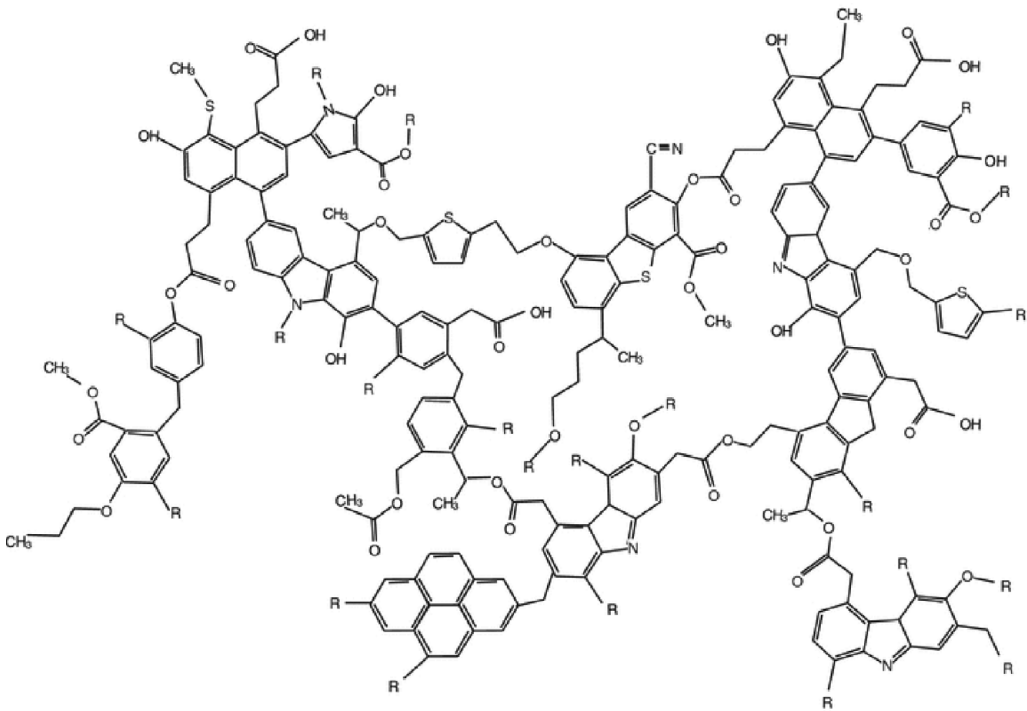


**Figure 13.** Model molecular structure of the IOM of Murchison meteorite. Figure adapted from Derenne & Robert (2010). This model is also applicable to the organic compound in PPN.

The strengths of the emission bands suggest that large quantities of organics are being synthesized and ejected into the interstellar medium. We now know that complex organics are commonly present in galaxies and they were produced in abundance in the early history of the Universe. Did evolved stars play an important role in the supply of organics in galaxies?

On the other side of the scale, is there a connection between organics produced by stars and those found in the Solar System? For this connection to exist, the organic grains have to survive in their journey through the ISM without extensive chemical processing either in the ISM or in the early Solar System. However, the discovery of pre-solar grains have confirmed that solid particles produced by AGB stars have reached the Earth (Zinner 1998). To what extent that the early Earth was enriched by organics from evolved stars (Kwok 2004, Kwok 2011) is an interesting topic for future studies.

### Acknowledgements

The work was supported by a grant from the Research Grants Council of the Hong Kong Special Administrative Region, China (Project No. HKU 7027/11P).

### References

- Alexander, C. M. O. D. 2011, these proceedings
- Alexander, C. M. O. D., Fogel, M., Yabuta, H., & Cody, G. D. 2007, *Geochimica et Cosmochimica Acta*, 71, 4380
- Allamandola, L. J., Tielens, A. G. G. M., & Barker, J. R. 1989, *ApJS*, 71, 733

- Allamandola, L. J., Hudgins, D. M., & Sandford, S. A. 1999, *ApJ*, 511, L115
- Cami, J. 2011, in *PAHs and the Universe*, eds. C. Joblin & A. G. G. M. Tielens, EAS Publications Series, 46, 117
- Cataldo, F., Keheyan, Y., & Heymann, D. 2002, *Int. J. Astrobiology*, 1, 79
- Cataldo, F. & Keheyan, Y. 2003, *Int. J. Astrobiology*, 2, 41
- Cataldo, F., Keheyan, Y., & Heymann, D. 2004, *Origins of Life and Evolution of the Biosphere*, 34, 13
- Cernicharo, J., Heras, A. M., Tielens, A. G. G. M., Pardo, J. R., Herpin, F., Gulín, M., & Waters, L. B. F. M. 2001, *ApJ*, 546, L123
- Clayton, G. C., *et al.* 2003, *ApJ*, 592, 947
- Colangeli, L., Mennella, V., Palumbo, P., Rotundi, A., & Bussoletti, E. 1995, *A&AS*, 113, 561
- Derenne, S. & Robert, F. 2010, *Meteoritics and Planetary Science*, 45, 1461
- Draine, B. T. & Li, A. 2007, *ApJ*, 657, 810
- Duley, W. W. & Williams, D. A. 1981, *MNRAS*, 196, 269
- Duley, W. W. & Hu, A. 2009, *ApJ*, 698, 808
- Evans, A., Tyne, V. H., Smith, O., Geballe, T. R., Rawlings, J. M. C., & Eyres, S. P. S. 2005, *MNRAS*, 360, 1483
- Flynn, G. J., Keller, L. P., Feser, M., Wirick, S., & Jacobsen, C. 2003, *Geochimica et Cosmochimica Acta*, 67, 4791
- Geballe, T. R., Tielens, A. G. G. M., Kwok, S., & Hrivnak, B. J. 1992, *ApJ*, 387, L89
- Guélin, M. 2011, these proceedings
- Guillois, O., Nenner, I., Papoular, R., & Reynaud, C. 1996, *ApJ*, 464, 810
- Hrivnak, B. J., Volk, K., & Kwok, S. 2000, *ApJ*, 535, 275
- Hrivnak, B. J., Geballe, T. R., & Kwok, S. 2007, *ApJ*, 662, 1059
- Hrivnak, B. J., Volk, K., & Kwok, S. 2009, *ApJ*, 694, 1147
- Hudgins, D. M. & Allamandola, L. J., 1999, *ApJ*, 516, L41
- Jäger, C., Huisken, F., Mutschke, H., Jansa, I. L., & Henning, T. H. 2009, *ApJ*, 696, 706
- Jones, A. P., Duley, W. W., & Williams, D. A. 1990, *Quart. J. Roy. Astr. Soc.*, 31, 567
- Keller, L. P., Messenger, S., Flynn, G. J., Clemett, S., Wirick, S., & Jacobsen, C. 2004, *Geochimica et Cosmochimica Acta*, 68, 2577
- Kerridge, J. F. 1999, *Sp. Sci. Rev.*, 90, 275
- Knacke, R. F. 1977, *Nature*, 269, 132
- Kwok, S. 1993, *Ann. Rev. Astr. Ap.*, 31, 63
- Kwok, S. 2000, *The Origin and Evolution of Planetary Nebulae*, CUP
- Kwok, S. 2004, *Nature*, 430, 985
- Kwok, S. 2011, *Organic Matter in the Universe*, Wiley
- Kwok, S., Volk, K., & Bidelman, W. P. 1997, *ApJS*, 112, 557
- Kwok, S., Volk, K. M., & Hrivnak, B. J. 1989, *ApJ*, 345, L51
- Kwok, S., Volk, K., & Hrivnak, B. J. 1999, *A&A*, 350, L35
- Kwok, S., Volk, K., & Bernath, P. 2001, *ApJ*, 554, L87
- Papoular, R. 2011, *MNRAS*, 415, 494
- Papoular, R., Conrad, J., Giuliano, M., Kister, J., & Mille, G. 1989, *A&A*, 217, 204
- Peeters, E., Hony, S., Van Kerckhoven, C., *et al.*, 2002, *A&A* 390, 1089
- Pilleri, P. *et al.* 2009, *MNRAS*, 397, 1053
- Prieto, J. L., Sellgren, K., Thompson, T. A., & Kochanek, C. S. 2009, *ApJ*, 705, 1425
- Puget, J. L. & Léger, A. 1989, *Ann. Rev. Astr. Ap.*, 27, 161
- Sakata, A., Wada, S., Onaka, T., & Tokunaga, A. T. 1987, *ApJ*, 320, L63
- Sandford, S. *et al.* 2006, *Science*, 314, 1720
- Scott, A. & Duley, W. W. 1996, *ApJ*, 472, L123
- Uchida, K. I., Sellgren, K., Werner, M. W., & Houdashelt, M. L. 2000, *ApJ*, 530, 817
- Van Kerckhoven, C., *et al.* 2000, *A&A*, 357, 1013
- Volk, K., Xiong, G.-Z., & Kwok, S. 2000, *ApJ*, 530, 408
- Volk, K. *et al.* 2011, *ApJ*, 735, 127
- Zhang, C. Y. & Kwok, S. 1991, *A&A*, 250, 179

Zhang, Y., Kwok, S., & Hrivnak, B. J. 2010, *ApJ*, 725, 990  
Zinner, E. 1998, *Ann. Rev. Earth Planet. Sci.*, 26, 147

## Discussion

DECIN: Prof. Kwok stated that PAH features were only detected in PPNe and PNe. Recently, K. Smolders *et al.* (2010) published the detection of PAH features in S type AGB stars, with a rich aliphatic component. This detection might help in understanding the excitation/formation of PAH.

KWOK: The AIB features in BZ CMa could be the result of a binary evolution. Thousands of AGB stars have been observed spectroscopically without showing AIB features.

HORNEKAER: Can you estimate the degree of impurities (N, O, S) in the carbon particles?

KWOK: O, N, S impurities are found in the IOM of meteorites but spectroscopic identification of heterocyclic aromatic compounds in astronomical sources will need much higher spectral resolution than is available at present.

STERNBERG: Do the solid-state features disappear before the nebula disperses? Does the appearance of the white dwarf affect the survival?

KWOK: As planetary nebulae expand, the flux of the infrared continuum also decreases as the result of geometric dilution of light from the central star. The strengths of the AIB features decreases correspondingly. As the central stars of PNe evolve to become WDs, the amount of UV light increases but there is no observed correlation between this and the strengths of the features.

MAUERSBERGER: Changes in proto-planetary nebulae spectra might be observed on a time scale of decades. It is therefore worthwhile to monitor such objects. This requires a thorough calibration and archiving of data.

KWOK: Since proto-planetary nebulae are evolving on time scales of  $10^2$ - $10^3$  yr, it would certainly be worthwhile to monitor changes in the infrared spectra at decade intervals.